

Mapping the antiparallel aligned domain rotation by microwave excitation

Jing Zhang(张景), Yuanzhi Cui(崔远志), Xiaoyu Wang(王晓雨), Chuang Wang(王创), Mengchen Liu(刘梦晨), Jie Xu(徐洁), Kai Li(李凯), Yunhe Zhao(赵芸鹤), Zhenyan Lu(陆振烟), Lining Pan(潘丽宁), Chendong Jin(金晨东), Qingfang Liu(刘青芳), Jianbo Wang(王建波), and Derang Cao(曹德让)

Citation: Chin. Phys. B, 2024, 33 (**9**): 097506. DOI: 10.1088/1674-1056/ad5536
Journal homepage: http://cpb.iphy.ac.cn; http://iopscience.iop.org/cpb

What follows is a list of articles you may be interested in

Effect of seed layers on the static and dynamic magnetic properties of CoIr films with negative effective magnetocrystalline anisotropy

Tianyong Ma(马天勇), Sha Zhang(张莎), Chenhu Zhang(张晨虎), Zhiwei Li(李志伟), Tao Wang(王涛), and Fashen Li(李发伸)

Chin. Phys. B, 2023, 32 (**12**): 127503. DOI: 10.1088/1674-1056/acd523

Magnetic anisotropy manipulation and interfacial coupling in $Sm_3Fe_5O_{12}$ films and CoFe/$Sm_3Fe_5O_{12}$ heterostructures

Lei Shen(沈磊), Guanjie Wu(武冠杰), Tao Sun(孙韬), Zhi Meng(孟智), Chun Zhou(周春), Wenyi Liu(刘文怡), Kang Qiu(邱康), Zongwei Ma(马宗伟), Haoliang Huang(黄浩亮), Yalin Lu(陆亚林), Zongzhi Zhang(张宗芝), and Zhigao Sheng(盛志高)

Chin. Phys. B, 2021, 30 (**12**): 127502. DOI: 10.1088/1674-1056/ac0040

Field-induced N\'eel vector bi-reorientation of a ferrimagnetic insulator in the vicinity of compensation temperature

Peng Wang(王鹏), Hui Zhao(赵辉), Zhongzhi Luan(栾仲智), Siyu Xia(夏思宇), Tao Feng(丰韬), and Lifan Zhou(周礼繁)

Chin. Phys. B, 2021, 30 (**2**): 027501. DOI: 10.1088/1674-1056/abbbef

Angular control of multi-mode resonance frequencies in obliquely deposited CoZr thin films with rotatable stripe domains

Chao-Zhong Li(李超众), Chang-Jun Jiang(蒋长军), and Guo-Zhi Chai(柴国志)

Chin. Phys. B, 2021, 30 (**3**): 037502. DOI: 10.1088/1674-1056/abccb4

Transformation behaviors, structural and magnetic characteristics of Ni–Mn–Ga films on MgO (001)

Xie Ren (谢忍), Tang Shao-Long (唐少龙), Tang Yan-Mei (唐妍梅), Liu Xiao-Chen (刘枭辰), Tang Tao (唐涛), Du You-Wei (都有为)

Chin. Phys. B, 2013, 22 (**10**): 107502. DOI: 10.1088/1674-1056/22/10/107502

Mapping the antiparallel aligned domain rotation by microwave excitation

Jing Zhang(张景)[1,2], Yuanzhi Cui(崔远志)[1,2,3], Xiaoyu Wang(王晓雨)[1,2], Chuang Wang(王创)[1,2], Mengchen Liu(刘梦晨)[1,2], Jie Xu(徐洁)[1,2], Kai Li(李凯)[1,2,†], Yunhe Zhao(赵芸鹤)[4], Zhenyan Lu(陆振烟)[5], Lining Pan(潘丽宁)[6], Chendong Jin(金晨东)[7], Qingfang Liu(刘青芳)[8], Jianbo Wang(王建波)[8,9], and Derang Cao(曹德让)[1,2,9,‡]

[1] *College of Physics, Qingdao University, Qingdao* 266071, *China*
[2] *National Demonstration Center for Experimental Applied Physics Education, Qingdao University, Qingdao* 266071, *China*
[3] *SKLSM, Institute of Semiconductors, Chinese Academy of Sciences, Beijing* 100083, *China*
[4] *College of Chemistry, Chemical Engineering and Resource Utilization, Northeast Forestry University, Harbin* 150040, *China*
[5] *Hunan Provincial Key Laboratory of Intelligent Sensors and Advanced Sensor Materials, School of Physics and Electronics, Hunan University of Science and Technology, Xiangtan* 411201, *China*
[6] *CAS Key Laboratory of Magnetic Materials and Devices, Ningbo Institute of Materials Technology and Engineering, Chinese Academy of Sciences, Ningbo* 315201, *China*
[7] *Key Laboratory of Optic-Electronic Information and Materials of Hebei Province, Research Center for Computational Physics, College of Physics Science and Technology, Hebei University, Baoding* 071002, *China*
[8] *Key Laboratory for Magnetism and Magnetic Materials of Ministry of Education, Lanzhou University, Lanzhou* 730000, *China*
[9] *Key Laboratory of Special Functional Materials and Structural Design, Ministry of Education, Lanzhou University, Lanzhou* 730000, *China*

(Received 20 March 2024; revised manuscript received 23 May 2024; accepted manuscript online 7 June 2024)

The evolution process of magnetic domains in response to external fields is crucial for the modern understanding and application of spintronics. In this study, we investigated the domain rotation in stripe domain films of varying thicknesses by examining their response to microwave excitation in four different orientations. The resonance spectra indicate that the rotation field of stripe domain film under an applied magnetic field approaches the field where the resonance mode of sample changes. The saturation field of the stripe domain film corresponds to the field where the resonance mode disappears when measured in the stripe direction parallel to the microwave magnetic field. The results are reproducible and consistent with micromagnetic simulations, providing additional approaches and techniques for comprehending the microscopic mechanisms of magnetic domains and characterizing their rotation.

Keywords: stripe domain, magnetic film, microwave excitation, micromagnetic simulation

PACS: 75.78.–n, 75.78.Fg, 76.50.+g, 75.70.Kw **DOI:** 10.1088/1674-1056/ad5536

1. Introduction

Stripe domain (SD) is an antiferromagnetic-like aligned magnetic domain structure found in soft magnetic films.[1] This structure is characterized by a striped appearance across the entire magnetic domain of the sample, with magnetic moments along the stripe direction showing uniform orientation, while the magnetic moments perpendicular to the stripe direction are arranged alternately, pointing either upward or downward in a periodic manner.[2–4] Such periodic SD leads to the formation of Bloch domain walls, Néel-type flux closure caps, and surface magnetization between two stripes.[4–7] The detailed magnetization distribution is shown in Fig. 1. The SD was initially discovered by Saito *et al.*[8] in permalloy ($Ni_{20}Fe_{80}$) prepared by thermal evaporation. However, due to the limitations of research methods at that time, for a long time the research was mainly focused on the static magnetic properties of SD films and their domain structures.[9–19] The magnetic domains were achieved using traditional magnetic force microscopy.

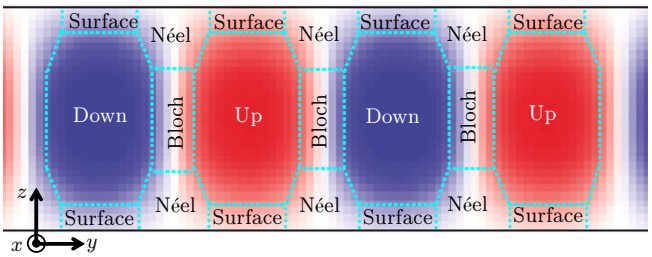


Fig. 1. Cross section of the magnetization distribution for an SD film over two periods obtained by micromagnetic simulation. The simulation dimensions are $1000\times1000\times150$ nm^3. The red (blue) color indicates a magnetization component in the positive z (negative z) direction. The SD is mainly composed of up-down basic domains, Bloch domain walls, Néel-type flux closure caps, and surface magnetization caps between two stripes.

In recent years, due to the special domain distribution of SD film, the study of SD has gained considerable theoretical and practical research interest.[6,19–25] For instance, by modifying parameters such as magnetic field, voltage, temperature, and mechanical stress, the magnetic structure

†Corresponding author. E-mail: kaili@qdu.edu.cn
‡Corresponding author. E-mail: caodr@qdu.edu.cn

© 2024 Chinese Physical Society and IOP Publishing Ltd

within these films can transition from SDs to topologically protected magnetic skyrmions.[26,27] Additionally, the SD film exhibits local magnetic domain-dependent multiple resonant modes and research on the microwave-excited magnetic properties of SD structure films has garnered considerable attention.[6,20,21,24,25,28] Currently, SD structures have been observed in films of FeNi,[14] Co,[29] FeCo,[30] NdCo,[9] FeBSi,[31] FeGa,[32] etc. Existing theoretical and experimental studies[5,14,33,34] have demonstrated that the appearance of SD results from the interplay among demagnetization energy, exchange energy, and perpendicular anisotropy energy in the soft magnetic film system. SD films exhibit numerous interesting and novel dynamic magnetic properties when compared to simple in-plane uniaxial anisotropy and out-of-plane uniaxial anisotropy films.[5,24,32,35]

First, SD structures exhibit reorientation behavior, wherein the direction of the SD is not fixed but can be realigned with the direction of an external magnetic field. Once the SD phase is formed, a pseudo-uniaxial anisotropy field appears along the stripe direction, and the direction of the anisotropy can be reoriented as the stripe direction changes. Therefore, a large number of researchers have focused on studying the control of SD rotational anisotropy.[1,13,22,30,32,36,37]

Second, SD structures possess rich microwave excitation resonance modes and can be selectively excited. Previous studies have shown[1,7,33,34] that when the SD is excited perpendicular to the direction of the microwave magnetic field (h_{rf}), an acoustic mode (AM) resonance occurs, with a resonance frequency similar to that of general uniaxial anisotropic soft magnetic films. However, when the SD is excited parallel to the h_{rf} direction, it undergoes an optical mode (OM) resonance, with a resonance frequency that can exceed twice the frequency of the AM resonance. Additionally, these two resonance modes are also accompanied by domain wall resonance and spin wave resonance modes.[5,19–21,24,25,32] This has sparked widespread interest among researchers in studying SD microwave-excited magnetic properties.[2,5,6,19–21,24,25,28,32,35] These prior studies have substantially enhanced our understanding of the theoretical and experimental aspects of static and high-frequency dynamic properties in SD films. However, there are few studies that focus on analyzing SD rotation using microwave techniques.

Here, we studied the microwave-excited magnetic properties of permalloy SD films with different thicknesses. The microwave excitation was performed in four orientations to fully characterize the evolution of SD under external magnetic fields. Static and dynamic micromagnetic simulations are in good agreement with experimental results, further confirming the reliability of describing SD rotation through microwave excitation.

2. Results and discussion

The permalloy films were deposited by radio frequency magnetron sputtering on a silicon wafer at room temperature. The sputtering power used was 140 W with an argon working pressure of 0.45 Pa. The thickness of films was controlled at 100 nm, 120 nm, 150 nm, 200 nm, and 300 nm, respectively. Magnetic force microscopy (MFM) measurements were conducted using an Asylum Research MFP3D instrument, revealing a well-defined pattern of SD structure in all films, as shown in Figs. 2(a)–2(e). It is evident that the stripe phase enhances and the stripe width of SD pattern broadens as the film thickness increases. It has been well-established previously[7,33,34] that the formation of SD is highly dependent on the film thickness, and the perpendicular anisotropy of the films increases due to the enhanced SD phase. The increasing stripe width is demonstrated to increase monotonically with the thickness t, either like $t^{1/3}$ [38] or $t^{1/2}$.[39]

Figure 2(f) displays the x-ray diffraction (XRD) patterns of the films, revealing a polycrystalline body-centered cubic (bcc) structure characterized by a prominent diffraction peak at (111) and two less pronounced diffraction peaks at (200) and (220), respectively. It is evident that the peak intensity rises with the film thickness, a phenomenon attributable to the increased volume of the diffracting material.[40]

The in-plane hysteresis loops of films measured by a vibrating sample magnetometer are depicted in Fig. 2(g). All the curves exhibit the typical feature of the SD film, with a linear variation of the magnetization (see the insert in Fig. 2(g)) between the coercivity and saturation fields.[5,7,32,35] This linear increase of the magnetization of film is attributed to the onset of a weak perpendicular anisotropy (i.e., out-of-plane magnetization component) in the SD film.[5,6] When the film thickness increases, the SD phase enhances in the film and the corresponding out-of-plane magnetization also increases. One can see from Fig. 2(h) that the remanence ratio M_r/M_s and saturation field H_s gradually decrease and increase, respectively, as the film thickness increases.

The microwave excitation measurements of the SD films were performed by a vector network analyzer-ferromagnetic resonance (VNA-FMR) system. The measurement orientations are shown in Figs. 3(a)–3(d). Four different configurations involving the microwave field h_{rf}, external magnetic field H, and SD were utilized to comprehensively describe the dynamic changes of SD film: (a) h_{rf} perpendicular to SD and H parallel to SD ($h_{rf}\perp$SD and $H\parallel$SD), (b) both h_{rf} and H perpendicular to SD ($h_{rf}\perp$SD and $H\perp$SD), (c) both h_{rf} and H parallel to SD ($h_{rf}\parallel$SD and $H\parallel$SD), (d) h_{rf} parallel to SD and H perpendicular to SD ($h_{rf}\parallel$SD and $H\perp$SD), respectively. Figures 3(a1)–3(d1) depict the resonance absorption spectra of 200 nm film in relation to the magnetic field H for the four test configurations. The detailed resonance absorption spectra

at the selected fields of 5 Oe, 450 Oe, and 720 Oe are, respectively, shown in Figs. 3(a2)–3(d2). The measurement results for the four configurations of other films (100 nm, 120 nm, 150 nm, and 300 nm) are shown in Fig. S1 of the supplementary material.

According to the Landau–Lifschitz–Gilbert (LLG) equation,[33] once the magnetization resonance is observed,[34] the pumping field h_{rf} must have a nonzero component perpendicular to the static magnetization $\boldsymbol{M}$ and exert a finite torque on the magnetization, causing it to tilt out of its equilibrium position, $\boldsymbol{M} \times \boldsymbol{h}_{rf} \neq 0$, or the total dynamic moment $\boldsymbol{m}_{tot}$ must have a nonzero projection parallel to the direction of the pumping field h_{rf}, $m_{tot} \cdot h_{rf} \neq 0$. We know from Fig. 1 that the magnetization of SD is comprised of four regions, corresponding to the basic up and down domain, the Bloch domain walls, the Néel-type flux closure caps, and the surface magnetization at the film.[2,32] The observation of the resonance absorption spectra in SD is determined by the magnetization proportion of these resonant regions.[5,34]

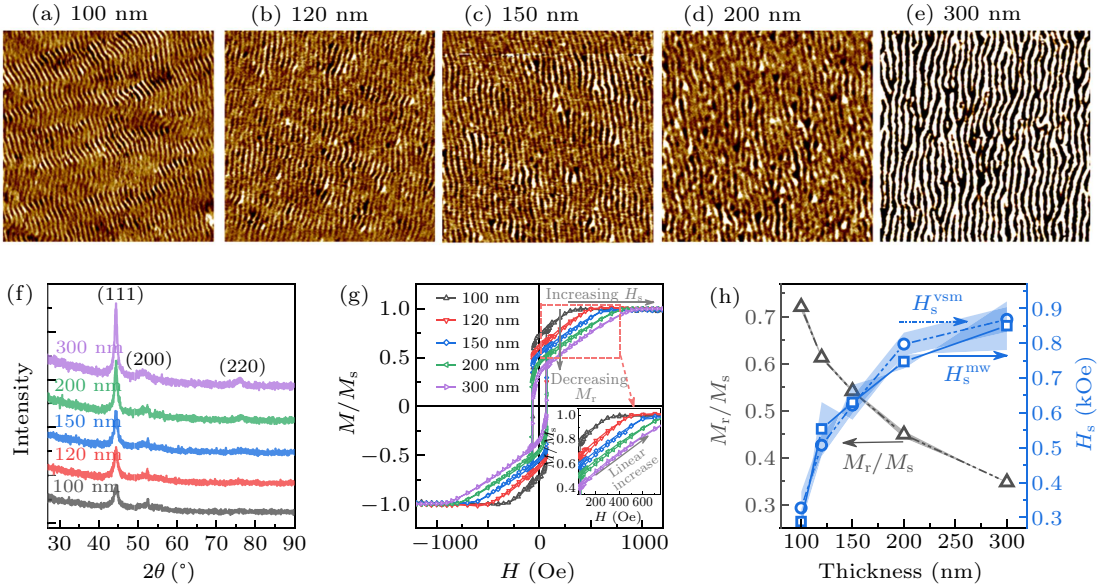


Fig. 2. (a)–(e) MFM images of the SD films probed at random positions. The image size is 10 μm×10 μm. (f) XRD spectra of SD films. (g) Hysteresis loop of SD films. The inset is an enlarged view of the area within the red dashed line. (h) Thickness dependence of normalized remanent magnetization (M_r/M_s) and saturation field (H_s) for SD films. The dashed line-circle data and solid line-square data are derived from hysteresis loops and the microwave-excited spectra, respectively.

Therefore, for the case of $h_{rf}\perp$SD and $H \parallel$SD as shown in Fig. 3(a1), the resonance belongs to mode AM. We observed a linear-like increase of resonance peak with increasing H. In this scenario, because the direction of SD aligns with H, the magnetization in the SD will increase linearly until saturation. Once the film magnetization reaches saturation, the SD pattern will disappear and a single domain is formed. The entire resonant process is similar to the uniform precessional Kittel mode.[4,6]

For the situation $h_{rf}\perp$SD and $H\perp$SD, as depicted in Fig. 3(b1), the microwave field is initially perpendicular to the SD and the resonance process mirrors that of mode AM shown in Fig. 3(a1). However, since the external magnetic field at this point is also perpendicular to the SD, the magnetization in the SD gradually rotates toward the direction of the increasing H. Once the H approaches H_{rot}, i.e., the magnetic field magnitude required for the SD to rotate to the H direction, the original AM resonance gradually disappears. Subsequently, the direction of the SD aligns parallel to both H and h_{rf}, and the OM resonance is observed. As the H increases, the magnetization in the SD increases linearly until saturation. Once the magnetization of the film is saturated (the magnetic field magnitude exceeds H_s), the film presents a single domain and the magnetization within the film is no longer disturbed by the microwave field. Consequently, no obvious resonance peak is observed. An example of the spectrum around H_s value of 720 Oe is presented in Fig. 3(b2).

When measuring the resonance absorption spectra under the condition $h_{rf} \parallel$SD and $H \parallel$SD, as shown in Fig. 3(c1), the resonance remains consistently in mode OM before H reaches the value of H_s. This entire process is similar to that of the mode OM case illustrated in Fig. 3(b1). However, we observe two resonance peaks when H is less than H_{rot}. The origin of the resonance has been demonstrated.[5,24,25,34] The higher peak originates from the resonance of the internal basic domain, while the other peak is from the resonance of domain walls. When the H exceeds H_{rot}, the magnetization within up-down basic domains in SD is mostly magnetized along the in-plane direction of H. The magnetization proportion from this part weakens, making it difficult to observe resonance peaks.

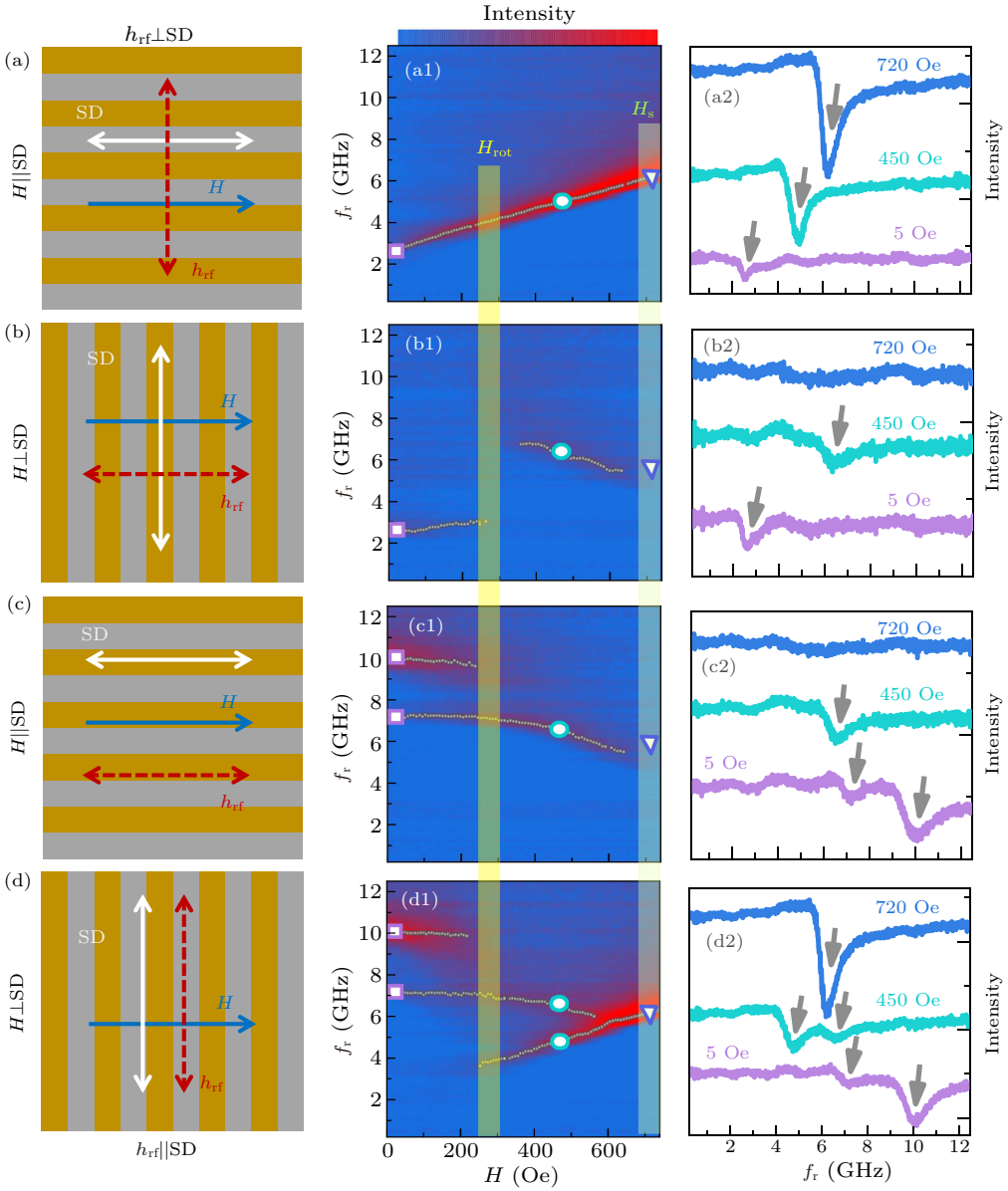


Fig. 3. (a)–(d) Four measurement orientations of the microwave excitation measurement. (a1)–(d1) Color-coded the resonance absorption spectra of 200 nm SD films as a function of the magnetic field H for the four configurations shown in (a)–(d). (a2)–(d2) Resonance absorption spectra at the selected fields of 5 Oe, 450 Oe, and 720 Oe, respectively. The arrows in (a2)–(d2) serve as guidelines for the observed resonance peak. The selected points are marked in (a1)–(d1).

For the case h_{rf} ||SD and H⊥SD as depicted in Fig. 3(d1), the same OM resonance as in Fig. 3(c1) is observed when the H is less than H_{rot}. However, when the H is larger than H_{rot} the SD rotates to the direction of H. At this time, the SD is perpendicular to h_{rf} and parallel to H. The AM mode is observed and the OM resonance gradually disappears. Once the film magnetization reaches saturation, the SD pattern disappears and a single domain forms. In this situation, all resonance modes of the film merge into one uniform precessional Kittel mode.

Combined with the results of the thickness dependence of microwave magnetic properties (shown in Fig. S1 of the supplementary material), the measurement results for the four configurations of other films (100 nm, 120 nm, 150 nm, and 300 nm) show the same tendencies and conclusions as those of the 200 nm film in Fig. 3. As observed from Fig. S1, with increasing film thickness, the values of H_{rot} and H_s increase and the resonance spectrum intensity of the samples strengthens. The increasing H_{rot} and H_s are attributed to the enhanced SD pattern (see MFM images in Fig. 2) with the increase in film thickness, resulting in increased perpendicular anisotropy. This enhanced SD phase also promotes an improvement in the magnetization proportion in domains and domain walls, leading to an increase in resonance intensity. We note that from the MFM pictures one can see that the SD phase is rather weak compared with other work.[2,5,6,24] This could result in a lower magnetization proportion of Bloch domain walls, the Néel-type flux closure caps, and surface magnetization in whole films.[1,4,5] Thus, we did not observe more resonance absorption peaks in this work.

The microwave-excited spectra of SD described above,

observed under four measurement orientations, phenomenologically elucidate the rotation and magnetization process of SD as the external magnetic field increases. One can conclude that the specified saturation field value in microwave excitation (H_s^{mw}) is very close to the H_s^{vsm} in VSM curves (see Fig. 2(h)). We note that it should use a static measurement method (i.e., *B*–*H* loop analyzer) to experimentally determine the H_{rot} by measuring the magnetization curves.[7] Specifically, the stripe direction is first fixed by applying a sufficiently large in-plane magnetic field along this direction and then removing it. Subsequently, the magnetic field is incrementally increased (starting from zero field) to measure the *B*–*H* loops in situations where the magnetic field is perpendicular and parallel to the initial direction of the SD, respectively. The intersection point of the two curves corresponds to H_{rot}. Since we have previously investigated the rotation field of SDs under an applied magnetic field in our prior work,[7] the detailed discussion is omitted here.

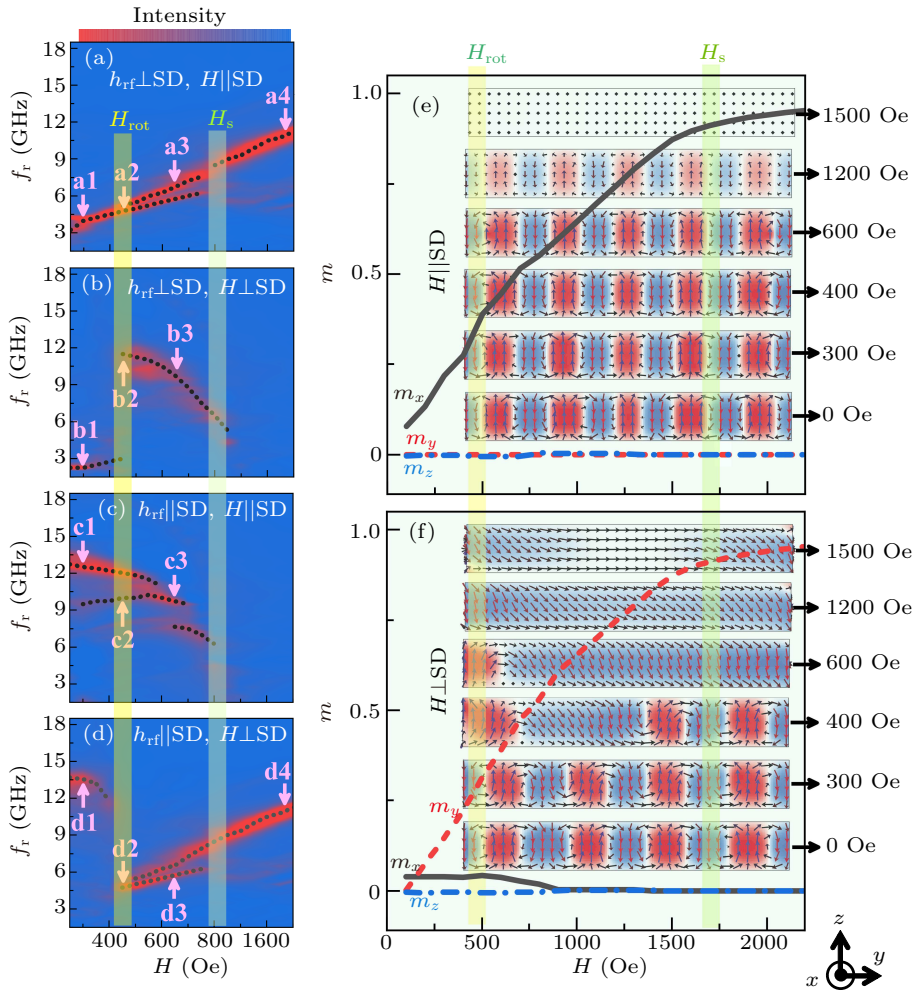


Fig. 4. Micromagnetic simulations. (a)–(d) Color-coded the resonance absorption spectra as a function of the magnetic field H for the four configurations shown in Figs. 3(a)–3(d). The labels a1–a4, b1–b3, c1–c3, and d1–d4 in (a)–(d) denote the selected applied magnetic fields and resonant frequencies corresponding to resonant mode in Fig. 5. (e) and (f) Magnetization (m_x, m_y, and m_z) dependent on the magnetic field H. The H is applied parallel to SD in (e) and perpendicular to SD in (f), respectively. The insert in (e) and (f) is the corresponding side view of the domain structure at representative different magnetic field H. Red and blue indicate a positive and negative magnetization component in the z direction, respectively. The arrows in (e) and (f) represent the direction of local magnetization.

To provide a more comprehensive description of this process, we conducted further studies on the domain structure and its microwave-excited spectra through micromagnetic simulations. The micromagnetic simulations were performed using the Mumax^3 software package.[41] The parameters used in the simulation are based on the analysis presented in Ref. [4]. The exchange stiffness constant A, the out-of-plane perpendicular anisotropy $K_\perp$, damping constant α, and saturation magnetization M_s were $A = 7.2\times10^7$ erg/cm, $K_\perp = 5.0\times10^5$ erg/cm^3, $\alpha = 0.01$, and $M_s = 10$ kGs, respectively. The magnetic volume is $1000\times1000\times150$ nm^3, which was discretized into cells of $5\times5\times5$ nm^3. In the model, the microwave excitation was applied using a sine pulse, $h(t) = h\sin[2\pi f(t-t)]/[2\pi f(t-t)]$ with an amplitude of $h = 10$ Oe, a frequency of $f = 50$ GHz, and a delay duration of $t = 100$ ps.

Figures 4(a)–4(d) show color-coded resonance absorption spectra that depend on the magnetic field H for the four configurations obtained through micromagnetic simulations. It is

evident that the simulation spectra are reproducible and consistent with the experimental observations. The change process of such resonance spectra aligns well with the rotation process of the SD. The evolution of SD with external magnetic field H is illustrated in Figs. 4(e) and 4(f). When H is parallel to SD (both H and SD on the x-axis, as seen in Fig. 4(e)), the SD direction remains unchanged while the magnetization component along x-axis (m_x) increases linearly with the increasing H until it reaches the saturation field H_s. The changes in SD can be obviously seen from the inserted domain structure. It should be noted that m_y and m_z are always approximately equal to zero as H increases. This is because the magnetization components in the y and z directions are always antisymmetric within a stripe period, leading to the cancelation of the total magnetization.

As shown in Fig. 4(f)), for the situation where H is perpendicular to SD (i.e., the initial direction of SD is along the x-axis and H is along y-axis), the magnetization component m_y increases with the increasing H before reaching H_s, while m_z remains around zero. However, the m_x slowly decreases with the increasing H, and then rapidly reduces to zero when the H is larger than H_{rot} ($\sim$ 500 Oe). This indicates the rotation process of SD, which is also reflected in the corresponding inserted domain structures. One can also intuitively observe the rotation process of SD from another perspective as shown in Fig. S2 of the supplementary material. Consequently, the magnetic field associated with the domain structure change can be well consistent with the magnetic field corresponding to the change of the resonance mode in the resonance spectra. We note that the magnetic domain distribution during SD rotation is relatively complex, and thus the resonance spectra in Figs. 4(a)–4(d) are a superposition of multiple resonance modes, making resonance peaks difficult to distinguish clearly.

To further identify each resonant mode shown in Figs. 4(a)–4(d), we investigated the magnetization component of the SD at different times by applying a sine-function magnetic field with varying resonance frequencies. The sinusoidal microwave magnetic field is expressed as $h(t) = h_0 \sin(2\pi f)$, where f is the resonance frequency of each resonant mode. The selection of the applied magnetic field matches the value range of H_{rot} and H_s to observe the resonance state after the SD rotation or saturation. Figures 5(a)–5(d) record the resonance modes for the four measurement configurations at selected applied magnetic fields and resonant frequencies. The results further confirm both the resonant origin and variation of each mode in SD with the increasing magnetic field, as discussed in Figs. 3 and 4.

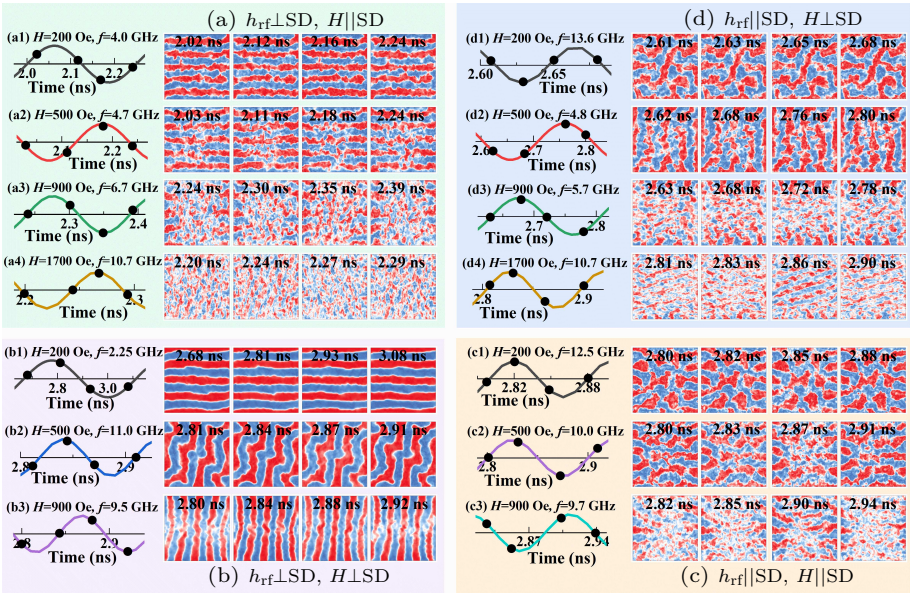


Fig. 5. Localization of typical resonance modes at selected applied magnetic fields and resonant frequencies corresponding to resonant spectra in Figs. 4(a)–4(d). The microwave magnetic fields are defined as $h(t) = h_0 \sin(2\pi f)$. (a)–(d) The left-hand side is the sine-function microwave magnetic field with the selected applied magnetic field and resonant frequency, and on the right-hand side are time snapshots of the m_z component of the SD excited by the sine-function microwave magnetic fields. Red and blue represent positive and negative magnetization components in the z direction, respectively. The times of the snapshots under the sine-function microwave magnetic field are indicated in the sine-function images on the left-hand side by the black solid circles.

3. Conclusion

We investigate the static and microwave-excited magnetic properties of SD structures with varying thicknesses. The microwave excitation test results under four orientations (microwave field, magnetic field, and SD direction) effectively illustrate the evolution of the stripe domain with the magnetic field, revealing distinctive microwave spectra at the stripe domain rotation magnetic field and the saturation magnetic field. These resonance absorption spectra offer novel approaches and techniques for characterizing magnetic domain rotation.

Acknowledgements

Project supported by the Natural Science Foundation of Shandong Province (Grant No. ZR2022MA053), the National Natural Science Foundation of China (Grant Nos. 11704211, 11847233, 52301255, 12205157, and 12205093), the Fundamental Research Funds for the Central Universities (Grant No. lzujbky-2022-kb01), China and Germany Postdoctoral Exchange Program (Helmholtz-OCPC), China Postdoctoral Science Foundation (Grant No. 2018M632608), and Applied Basic Research Project of Qingdao (Grant No. 18-2-2-16-jcb).

References

[1] Ebels U, Buda L D, Ounadjela K and Wigen P E 2002 *Spin Dynamics in Confined Magnetic Structures I*, Hillebrands B and Ounadjela K eds. (Berlin, Heidelberg: Springer) pp. 167–217
[2] Banerjee C, Gruszecki P, Klos J W, Hellwig O, Krawczyk M and Barman A 2017 *Phys. Rev. B* **96** 024421
[3] Dürr H A, Dudzik E, Dhesi S S, Goedkoop J B, van der Laan G, Belakhovsky M, Mocuta C, Marty A and Samson Y 1999 *Science* **284** 2166
[4] Yu J, Chen X, Wang F, Adam R, Bürgler D E, Pan L, Zhang J, Cui Y, Li Q, Liu M, Xu J, Li S, Parlak U, Wang J, Liu Q, Cinchetti M, Schneider C M and Cao D 2023 *New J. Phys.* **25** 013008
[5] Ben Youssef J, Vukadinovic N, Billet D and Labrune M 2004 *Phys. Rev. B* **69** 174402
[6] Li Q, Song Y, Wang F, Liu M, Ma X, Guo X, Chen X, Yu J, Du S, Li H, Xu J, Li S and Cao D 2022 *J. Phys.: Condens. Matter* **34** 155802
[7] Liu M, Li Q, Song C, Feng H, Song Y, Zhong L, Pan L, Zhao C, Li Q, Xu J, Li S, Wang J, Liu Q and Cao D 2022 *J. Magn. Magn. Mater.* **547** 168939
[8] Saito N, Fujiwara H and Sugita Y 1964 *J. Phys. Soc. Jpn.* **19** 1116
[9] Hierro-Rodriguez A, Cid R, Vélez M, Rodriguez-Rodriguez G, Martín J I, Álvarez-Prado L M and Alameda J M 2012 *Phys. Rev. Lett.* **109** 117202
[10] Chen G, Zhu J, Quesada A, Li J, N'Diaye A T, Huo Y, Ma T P, Chen Y, Kwon H Y, Won C, Qiu Z Q, Schmid A K and Wu Y Z 2013 *Phys. Rev. Lett.* **110** 177204
[11] Bručas R, Hafermann H, Katsnelson M I, Soroka I L, Eriksson O and Hjörvarsson B 2004 *Phys. Rev. B* **69** 064411
[12] Amos N, Fernandez R, Ikkawi R, Lee B, Lavrenov A, Krichevsky A, Litvinov D and Khizroev S 2008 *J. Appl. Phys.* **103** 07E732
[13] Fin S, Tomasello R, Bisero D, Marangolo M, Sacchi M, Popescu H, Eddrief M, Hepburn C, Finocchio G, Carpentieri M, Rettori A, Pini M G and Tacchi S 2015 *Phys. Rev. B* **92** 224411
[14] Voltan S, Cirillo C, Snijders H, Lahabi K, García-Santiago A, Hernández J, Attanasio C and Aarts J 2016 *Phys. Rev. B* **94** 094406
[15] Wang G, Dong C, Wang W, Wang Z, Chai G, Jiang C and Xue D 2012 *J. Appl. Phys.* **112** 093907
[16] Yang S, Moon K W, Ju T S, Kim C, Park S and Hwang C 2021 *J. Magn. Magn. Mater.* **539** 168381
[17] Oukaci K A, Lacour D, Stoeffler D, Sarpi B, Montaigne F, Belkhou R and Hehn M 2020 *Phys. Rev. Appl.* **14** 024083
[18] Dai G, Xing X, Shen Y and Deng X 2020 *J. Phys. D: Appl. Phys.* **53** 055001
[19] Pianciola B, Flewett S, De Biasi E, Hepburn C, Lounis L, Vasquez-Mansilla M, Granada M, Barturen M, Eddrief M, Sacchi M, Marangolo M and Milano J 2020 *Phys. Rev. B* **102** 054438
[20] Grassi M, Geilen M, Oukaci K A, Henry Y, Lacour D, Stoeffler D, Hehn M, Pirro P and Bailleul M 2022 *Phys. Rev. B* **105** 094444
[21] Liu C, Wu S, Zhang J, Chen J, Ding J, Ma J, Zhang Y, Sun Y, Tu S, Wang H, Liu P, Li C, Jiang Y, Gao P, Yu D, Xiao J, Duine R, Wu M, Nan C W, Zhang J and Yu H 2019 *Nat. Nanotech.* **14** 691
[22] Salikhov R, Samad F, Boehm B, Schneider S, Pohl D, Rellinghaus B, Ullrich A, Albrecht M, Lindner J, Kiselev N S and Hellwig O 2021 *Phys. Rev. Appl.* **16** 034016
[23] Nakane R, Hirose A and Tanaka G 2021 *Phys. Rev. Research* **3** 033243
[24] Camara I S, Tacchi S, Garnier L C, Eddrief M, Fortuna F, Carlotti G and Marangolo M 2017 *J. Phys.: Condens. Matter* **29** 465803
[25] Vukadinovic N and Youssef J B 2019 *Phys. Rev. B* **100** 224423
[26] Gao Y, Zhang J, Dou P, Li Z, Zhu Z, Guo Y, Hu C, Qin W, He C, Shen S, Zhang Y and Wang S 2022 *Chin. Phys. B* **31** 067502
[27] Wang Z, Liang J and Yang H 2023 *Chin. Phys. Lett.* **40** 017501
[28] Wang W, Wang F, Cao C, Li P, Yao J and Jiang C 2018 *J. Phys. D: Appl. Phys.* **51** 145002
[29] Donzelli O, Bassani M, Spizzo F and Palmeri D 2008 *J. Magn. Magn. Mater.* **320** e261
[30] Chai G, Phuoc N N and Ong C K 2013 *Appl. Phys. Lett.* **103** 042412
[31] Coïsson M, Celegato F, Olivetti E, Tiberto P, Vinai F and Baricco M 2008 *J. Appl. Phys.* **104** 033902
[32] Tacchi S, Fin S, Carlotti G, Gubbiotti G, Madami M, Barturen M, Marangolo M, Eddrief M, Bisero D, Rettori A and Pini M G 2014 *Phys. Rev. B* **89** 024411
[33] Vukadinovic N, Vacus O, Labrune M, Acher O and Pain D 2000 *Phys. Rev. Lett.* **85** 2817
[34] Ebels U, Buda L, Ounadjela K and Wigen P E 2001 *Phys. Rev. B* **63** 174437
[35] Liu M, Du S, Wang F, Adam R, Li Q, Ma X, Guo X, Chen X, Yu J, Song Y, Xu J, Li S and Cao D 2021 *J. Alloys Compd.* **869** 159327
[36] Tee Soh W, Phuoc N N, Tan C and Ong C 2013 *J. Appl. Phys.* **114** 053908
[37] Ma X, Zhan Q, Li J, Liu Q, Wang B and Li R 2018 *Acta Metallurgica Sinica* **54** 1281
[38] Murayama Y 1966 *J. Phys. Soc. Jpn.* **21** 2253
[39] Hubert A and Schäfer R 2008 *Magnetic domains: the analysis of magnetic microstructures*, 3rd edn. (New York: Springer Science & Business Media) p. 299
[40] Kumari T P, Raja M M, Kumar A, Srinath S and Kamat S V 2014 *J. Magn. Magn. Mater.* **365** 93
[41] Vansteenkiste A, Leliaert J, Dvornik M, Helsen M, Garcia-Sanchez F and Waeyenberge B V 2014 *AIP Adv.* **4** 107133